

LiDAR mapping of the Snæfellsjökull ice cap, western Iceland

Tómas Jóhannesson¹, Helgi Björnsson², Finnur Pálsson²,
Oddur Sigurðsson¹ and Þorsteinn Þorsteinsson¹

¹*Icelandic Meteorological Office, Bústaðavegur 9, IS-150 Reykjavík, Iceland*

²*Institute of Earth Sciences, University of Iceland, Askja, IS-107 Reykjavík, Iceland*

Corresponding author: tj@vedur.is

Abstract — *The surface of the Snæfellsjökull ice cap in western Iceland was mapped with airborne LiDAR in 2008. A comparison with a DTM from 1999 derived by aerial photogrammetry shows that the surface of the ice cap has been lowered by 14.0 m on average during this nine year period, corresponding to an annual average mass loss of 1.25 m_{w.e.} per year when a correction has been made for the different timing of the LiDAR survey and the aerial photographs. The area of the ice cap was reduced from 12.5 km² in 2002 to 10.0 km² in 2008. Based on meteorological observations at Stykkishólmur, ~60 km to the east of the ice cap, the ice volume reduction indicates a mass balance sensitivity of $-1.9 \text{ m}_{\text{w.e.}} \text{ a}^{-1} \text{ }^{\circ}\text{C}^{-1}$ for the ice cap. This is within the range of sensitivities estimated for other ice caps and glaciers in Iceland in recent years. As the average ice thickness of Snæfellsjökull is only 30 m, most of the ice cap is likely to disappear within a few decades if the warm climate of Iceland in recent years persists. The LiDAR DTM has been successfully used to delineate the location of crevasses with an automated procedure based on the calculation of the local curvature of the ice surface.*

INTRODUCTION

The picturesque Snæfellsjökull (Figure 1) is the only ice cap that can be seen from the capital of Iceland, Reykjavík. It has persisted for many centuries, at least since Iceland was settled in the ninth century AD. The extent of the ice cap varied substantially during the 20th century with rapid retreat in the warm period 1930–1965, a partial readvance in the cooler period 1970–1995, and retreat since 1995 (Figure 2), similar as for many other non-surge-type glaciers in Iceland (Sigurðsson and Jóhannesson, 1998). The area of the ice cap in 2002 was 12.5 km² and the average thickness was measured to be only ~30 m in 2003, reaching 60–90 m in the main outlet tongues, Blágilsjökull, Jökulháls and Hyrningsjökull (Davíðsdóttir, 2003).

There have been few scientific studies of Snæfellsjökull except for regular measurements of the variations of several termini since 1931 (Sigurðsson, 1998) and the measurements of Davíðsdóttir and co-workers (2003) which included radio echo-sounding of the ice thickness and GPS-measurements of ice surface elevation on several profiles across the ice cap. The terminus measurements were initially conducted at five locations but after 1957 only the measurements of Hyrningsjökull on the east side of the ice cap have provided a consistent record of terminus variations. Measurements were also conducted at Jökulháls on the northeastern side of the ice cap in some years after 1957. The terminus there was inactive and frequently covered by snow year round so the record from that location does not indicate true variations of



Figure 1. Snæfellsjökull seen from the east. The location of the outlet glaciers mentioned in the text is indicated on the photograph. – *Snæfellsjökull frá austri. Skriðjökklar sem minnst er á í greininni eru nefndir á myndinni.* Photo: *Ljósmynd Oddur Sigurðsson, 2001.*

the glacier terminus until 1998 when glacier ice was exposed at the terminus and measurements at Jökulháls were again reported in the annual reports of the Iceland Glaciological Society (Sigurðsson, 2009).

The area of the ice cap was 22 km² in 1910 according to maps of Iceland published by the Danish General Staff (Björnsson, 1978). The outline of the glacier drawn on the AMS maps of the US Army Map Service indicates that the area had shrunk to 16 km² in 1946, and in 1960 it was only 11 km² according to an analysis of aerial photographs (Björnsson, 1978). More recently, the area has been measured in the field by differential GPS-measurements by Bjarni Reykr Kristjánsson and delineated on SPOT5 images and with the aid of the LiDAR measurements described here. These more recent measurements are tabulated in Table 1 together with the older area estimates showing that the area of the glacier in 2008 had been reduced below the low 1960 value.

The earlier area estimates from 1910 and 1946, based on maps, must be considered uncertain as systematic delineation of the ice margin was not carried out as a part of the preparation of the maps. The estimated area in 1910, in particular, is likely to have included some snow-covered areas adjacent to the ice cap that are unlikely to have been covered by glacier ice. However, the variations in the area shown in Table 1 are not inconsistent with the terminus variations of Hymningsjökull shown in Figure 2 and climatic variations in Iceland since the end of the Little Ice Age. If the area in 1910 given in Table 1 is assumed to be correct, ice-volume–area scaling, $v = cs^\gamma$, where v and s are ice volume and area, respectively, and c and γ are coefficients (Bahr, 1997) may be used (with $\gamma = 1.25$ which is appropriate for ice caps) to estimate that more than 60% of the ice volume of Snæfellsjökull has been lost since the beginning of the 20th century.

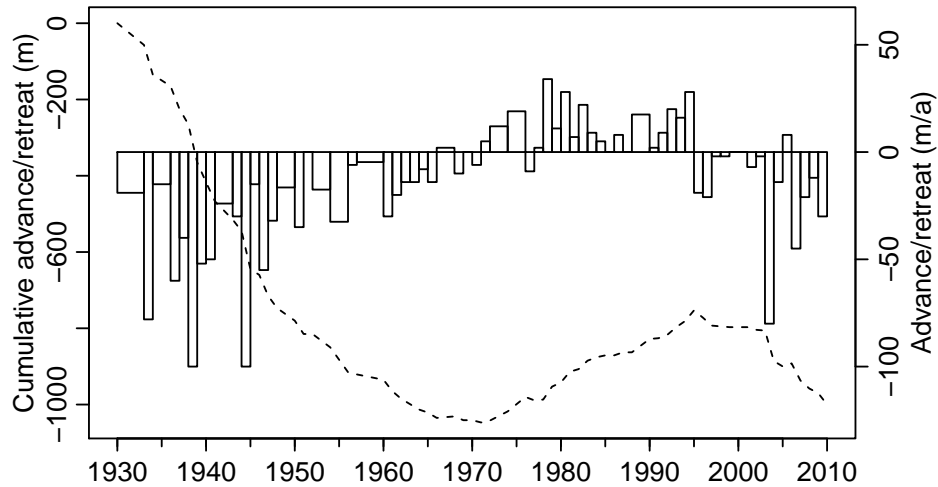


Figure 2. Annual advance and retreat of the Hyrningsjökull outlet glacier on the east side of Snæfellsjökull from 1931–1932 to 2009–2010 (bars) and the cumulative variation of the terminus since 1931 (dashed curve) (data from the database of the Iceland Glaciological Society). The ticks on the x-axis separate the measurement intervals (*i.e.* the tick marked “1960” is at the end of the interval 1959/60 and at the beginning of the interval 1960/61 which is in the fall of 1960). Measurements are missing from some years in which case the width of the bar indicates the number of years that elapsed between measurements and the height of the bar indicates the average annual advance or retreat. – *Breytingar á Hyrningsjökli (skriðjökull til austurs úr Snæfellsjökli) á tímabilinu 1931–1932 til 2009–2010 (stöplarit) og heildarbreyting á stöðu jökulsporðsins síðan mælingar hófust 1931 (slitinn ferill). Hökin á x-ásnum sýna upphaf og endi mælitímabilanna (þ.e. hakið sem merkt er „1960“ sýnir endi mæliársins 1959/60 og upphaf mæliársins 1960/61).*

Table 1. Measurements and estimates of the area of Snæfellsjökull. – *Flatarmál Snæfellsjökuls.*

Year	Area (km ²)	Source
1910	22	Map of the Danish General Staff
1946	16	AMS-map, published 1949/50
1960	11	Aerial photographs (Björnsson, 1978)
2002	12.5	Field GPS-measurements by Bjarni Reyr Kristjánsson
2006	11.1	SPOT5
2008	10.0	LiDAR map

Note: Björnsson and Pálsson (2008) list the area, ice volume and other characteristics of Snæfellsjökull as well as for many other glaciers and ice caps in Iceland. The tabulated quantities for Snæfellsjökull are said to refer to the year ~2000 in their table. However, the area of 16 km² for Snæfellsjökull refers to the outline of the glacier on the AMS maps based on aerial photographs from 1946 whereas the values for the ice volume and average ice thickness are based on the above-mentioned measurements of Davíðsdóttir and co-workers in 2003.

Aerial photographs from 1999 by Loftmyndir ehf. have been used to derive a comparatively accurate map of the ice surface elevation of that year. Manually drawn elevation contours by Hnit hf. based on aerial photographs from 1979 and elevation contours from the AMS maps based on aerial photographs from 1946 may also be used to estimate the ice surface elevation of those years but the accuracy of those surface maps is limited by the known problems of measuring elevations of snow covered surfaces by traditional photogrammetric methods. No mass balance measurements have been made on Snæfellsjökull but some bounds on the cumulative mass balance of the whole ice cap for extended periods may be derived from the ice surface elevation from the Hnit and AMS maps and more recent measurements of the surface of the ice cap that are described here.

Meteorological measurements were conducted at a research station at 820 m a.s.l. on the northeastern side of Snæfellsjökull for eleven months as a part of the International Polar Year 1932–1933 (Kristjánsson and Jónsson, 1998; Zingg, 1941). The station collected meteorological and various geophysical data, including daily temperature and precipitation but no glaciological measurements were carried out.

As a part of and in continuation of the International Polar Year (IPY) 2007–2009, accurate Digital Terrain Models (DTMs) of Icelandic ice caps are being produced with airborne LiDAR technology. It is important that the glaciers are accurately mapped now when rapid changes have started in response to warming climate. Mapping of glacier surfaces may be accomplished by use of several remote sensing methods. The most advanced in terms of resolution and vertical accuracy is airborne LiDAR. Satellite acquired data is more cost efficient, but yields less horizontal resolution and vertical accuracy (by a factor of 2–10). An advantage of airborne LiDAR for mapping of glaciers is that crevassed areas and other areas on the glaciers that are difficult to access on land can easily be measured with high accuracy. Snæfellsjökull, Eiríksjökull and most of Hofsjökull were mapped in 2008.

This paper describes the results of the LiDAR mapping of Snæfellsjökull, comparing the ice surface elevation with earlier measurements from 1999

and interpreting the obtained ice volume changes in terms of climate variations at the nearby Stykkishólmur weather station. Use of the new LiDAR maps for automated mapping of crevassed areas is also briefly discussed.

DATA

The two DTMs of Snæfellsjökull that are compared here were acquired by an airborne LiDAR operated by the German mapping company TopScan GmbH on 2 September 2008 and by the Icelandic company Loftmyndir ehf. on 5 August 1999 using aerial photogrammetry based on photographs taken from an altitude of 3000 m. The LiDAR measurements were carried out with an Optech ALTM 3100 laser scanner from an altitude of 2500 m above ground with a 1300 m distance between flight lines and a swath width of 1819 m. The wavelength of the ALTM LiDAR is 1064 nm. A GPS base station for kinematic correction of the on-board GPS instrument was operated at the ISNET triangulation network point LM0313 (Hellissandur/Rif), about 30 km from the summit of the ice cap. The average measurement point density was 0.33 m^{-2} , *i.e.* approximately one measurement every 3 m^2 . The measurements were averaged and interpolated onto a regular $5 \times 5 \text{ m}$ grid using the SCOP.DTM software (TU-Vienna-IPF, 2002).

Two measurements are obtained from each reflected laser pulse corresponding to the first and the last returned pulse. The measurements corresponding to the first pulse were used to calculate the regular DTM as these are considered more likely to originate from the “smooth” ice surface that the DTM is intended to represent. The last pulse measurements, which may be expected to be more affected by surface irregularities such as crevasses and melt channels, may be used together with the first pulse measurements in special purpose studies such as digital delineation of crevasses or geomorphological analysis.

GPS validation measurements are carried out in the field on a day close to the timing of the aerial surveys on each glacier mapped in the LiDAR mapping effort. Validation measurements were made along a $\sim 1 \text{ km}$ long line near the ice margin north of the Hyrningsjökull outlet glacier and they are compared

with the 5x5 m LiDAR DTM and with a local least squares fit using the more dense, randomly distributed point measurements from which the DTM is derived in Figure 3. The magnitude of the differences with respect to the DTM is less than ~ 0.5 m in all cases, and less than ~ 0.3 – 0.4 m with respect to the local fit to the LiDAR point measurements, with a median of ~ 0.2 m (negative bias in the LiDAR DTM), indicat-

ing a vertical accuracy well within the intended range of ± 0.5 m. The differences with respect to the local fit to the LiDAR point measurements are consistently smaller than the differences with respect to the 5x5 m DTM. This indicates that small variations in the surface geometry on shorter length-scales than captured by the 5x5 m DTM are consistently resolved by the more dense point measurements. Part of the nega-

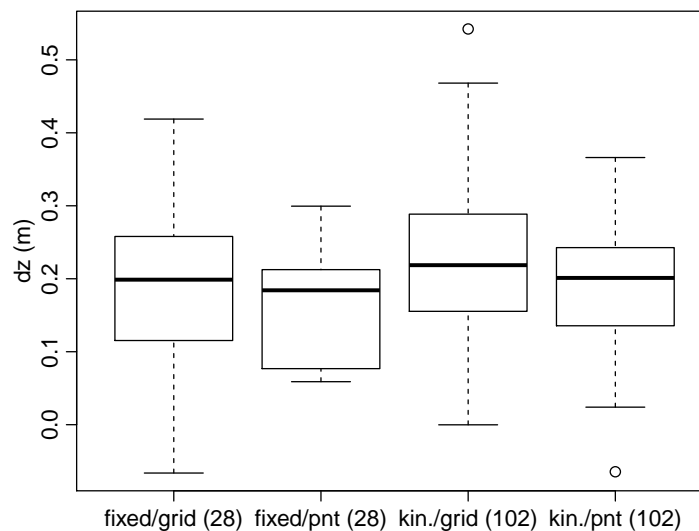


Figure 3. Differences between GPS validation measurements and the 5x5 m LiDAR DTM (labelled “grid” on the plot) and a local least squares fit using the more dense, randomly distributed point measurements within a distance of 2–4 m from the GPS-points (labelled “pnt”) (GPS-measurements minus the LiDAR measurements). The surface elevation was measured with a differential GPS-instrument 4 days after the aerial LiDAR survey on 2 September 2008. The box-plots show 28 GPS-measurements taken with a ~ 15 sec. occupation of the GPS-instrument at the points (the two box-plots labelled “fixed” on the plot), ensuring cm-scale accuracy, and 102 measurements taken in continuous kinematic mode in transit between the 28 points (the two box-plots labelled “kin.”), respectively. The latter measurements have somewhat worse accuracy but are nevertheless accurate to within a decimetre. The thick line shows the median of the differences, the box encloses 50% of the differences and the whiskers extend out to the most extreme data points (but no longer than 1.5 times the interquartile range). – *Skekkja 5x5 m landlíkansins (merkt „grid“ á lárétta ásnun) og minnstu kvadrata greiningar á upprunalegu LiDAR mælingunum (merkt „pnt“ á lárétta ásnun) í punktum þar sem landhæð var mæld fjórum dögum eftir LiDARflugið í september 2008. Sýnd er dreifing skekkjunnar í 28 punktum þar sem hæð var mæld með fullri nákvæmni GPS-landmælingatækisins (nákvæmni upp á nokkra cm) og í 102 punktum til viðbótar sem mældir voru á ferð milli punktanna 28 með heldur lakari nákvæmni (skekkja í þessum punktum getur verið allt að 10 cm). Breið þverstrík sýna miðgildi skekkjunnar, kassarnir umlykja 50% gildanna og hökin teiknast út í ystu gildin en þó ekki lengra en sem nemur 1.5 sinnum hæð kassans frá miðgildinu.*

tive bias may be due to compressive ice deformation over the four days that elapsed between the aerial survey and the GPS-measurements, which would tend to raise the ice surface slightly during this time of the year when summer melting is mostly over. However, as the bias is of similar magnitude outside the ice margin, it is most likely that the negative bias is the result of a small bias in the LiDAR measurements, which is well within the expected error of the measurements.

The Loftmyndir DTM is based on digital processing of aerial photographs from a flight altitude of 3000 m. The 10x10 m DTM was reprocessed for the purpose of this study using new GPS-measurements of distinguishable features from ice-free areas around the ice margin to improve the vertical accuracy. The

surface elevation according to the 1999 and 2008 DTMs along eleven profiles across the ice cap from west to east shows that the DTMs are consistent in ice-free areas (Figure 4). The consistent variations of the 1999 and 2008 DTMs within the ice margin indicate that the digital stereoscopic processing of the aerial photographs from 1999 successfully identified the ice- and snow-covered surface of the glacier. The surface of Snæfellsjökull in the fall is comparatively suitable for stereoscopic processing of aerial photographs due to numerous nunataks and ice-free ridges, dust blown onto the glacier from the barren lands outside the ice margin and dense crevasse patterns that provide visual features that aid the stereoscopic processing.

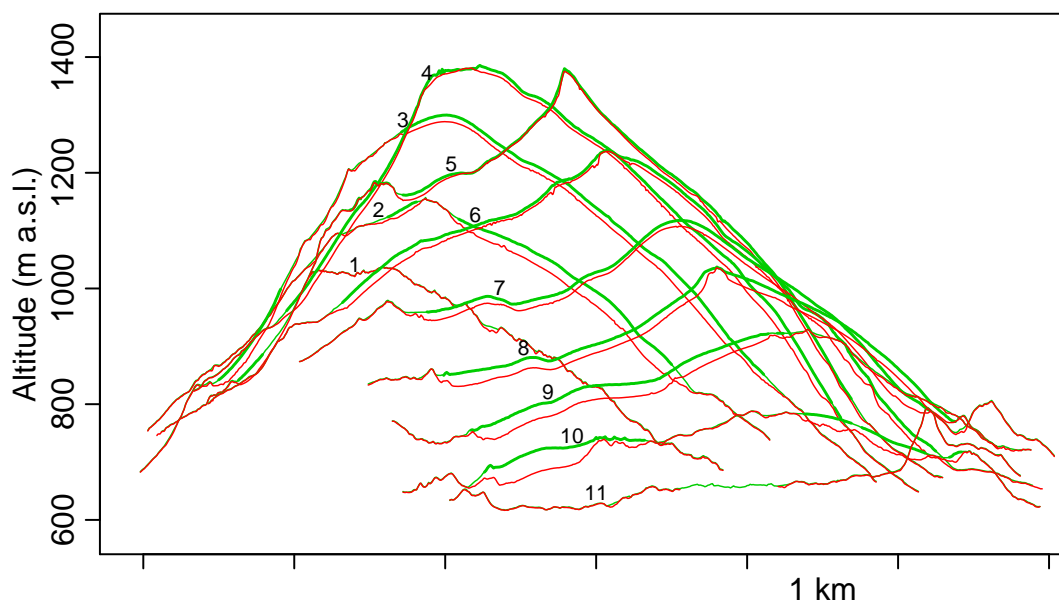


Figure 4. Measured elevation in 1999 (green) and 2008 (red) on eleven profiles crossing the ice cap from west to east (see Figure 6 for the map location of the profiles). The part of the profiles that is within the 2002 ice margin is drawn with a thicker curve on the 1999 profile. The profiles are progressively shifted to the east as indicated by the horizontal location of the numerical labels to reduce overplotting. – Landhæð eftir ellefu sniðum frá vestri til austurs yfir jökulinn (lega sniðanna er sýnd á mynd 6). Grænir ferlar sýna mælingar Loftmynda ehf. frá 1999 en rauðir ferlar LiDAR mælingar TopScan haustið 2008. Sá hluti sniðanna frá 1999 sem er innan jökuljádarsins frá 2002 er dreginn með breiðum ferli. Sniðunum er hliðrað jafnt og þétt til austurs eftir því sem númer þeirra hækkar til þess að þau skiljist betur að á myndinni.

A detailed comparison of the 1999 Loftmyndir DTM with the LiDAR DTM in ice-free areas around the ice margin indicates a ~ 1.0 m one-sided bias (mean 1.0 m, median 0.9 m). This comparison was carried out by masking out snow covered areas outside the ice margin in 1999 based on a rectified 1999 aerial photograph (Figure 5, left). This leaves ~ 70 thousand points on which the estimation of the bias is based. After the subtraction of this bias, the differences between ice-free areas of the DTMs were unbiased and less than 0.5 m in magnitude at more than 50% of the considered points. Several metres differences were found in $\sim 1\%$ of the points and >10 m differences in $\sim 0.1\%$ of the points, as may be expected

in a landscape with gullies, ridges and other sharp features that are not resolved in the 5x5 m and 10x10 m DTMs. Comparison of the DTMs in several hand-picked ice-free areas outside the ice margin, on three nunataks within the northern part of the glacier and along the ice free part of the profiles in Figure 4 indicates a similar value of the bias on all sides of and within the ice cap. Based on this analysis, 1.0 m was subtracted from the Loftmyndir DTM before the calculation of the thinning of the ice cap discussed in the next section.

The 1999 orthophoto of Snæfellsjökull with the GPS-measurement of the ice margin in 2002 is shown in Figure 5 (left panel) together with a hillshade of the

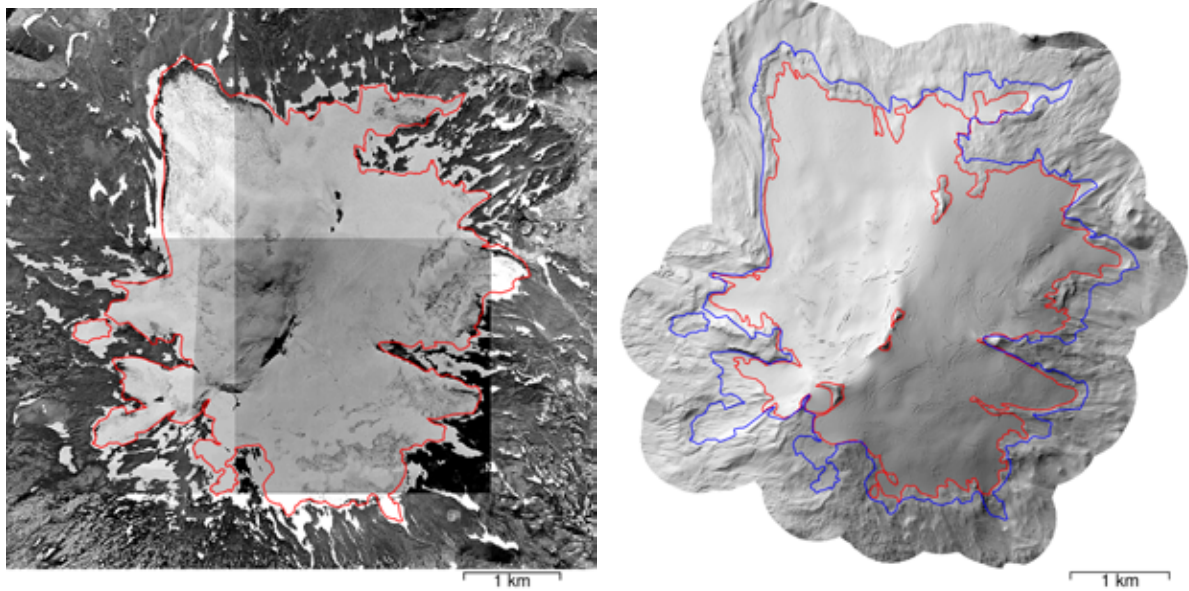


Figure 5. Left: Orthophoto of Snæfellsjökull from 5 August 1999 (© Loftmyndir ehf.). The glacier margin measured by GPS in the field in 2002 shown with a red curve is close to the location of the ice margin in 1999. Right: A hillshade of the 2008 LiDAR digital elevation model. The glacier margin in 2008 as delineated from the LiDAR measurements and the 2002 margin measured by GPS are shown with red and blue curves, respectively. Note that the outline close to the ice margin is shown with a red curve in both pictures. The 2002 outline measured by GPS is shown with a red curve on the left and a blue curve on the right. – *Vinstri mynd: Upprätt loftmynd af Snæfellsjökli frá 5. ágúst 1999 (© Loftmyndir ehf.). GPS-mæling á útlínu jökulsins frá 2002 er sýnd með rauðri línu. Hægri mynd: Skygging á LiDAR landlíkaninu frá 2008. Útlína jökulsins frá 2008 dregin á grundvelli LiDAR mælingarinnar er sýnd með rauðri línu og útlínan frá 2002 með blárrí línu.*

2008 DTM with the 2002 ice margin and as well as an estimate of the location of the ice margin in 2008 derived from the LiDAR measurements (right panel).

The hillshade in Figure 5 shows surface features on the glacier such as crevasses and undulations due to ice flow over bedrock topography and various geomorphological features in the forefield of the glacier in great detail due to the high resolution and good internal consistency of the LiDAR measurements. The different texture of the ice-covered and ice-free surfaces that may be differentiated on the hillshade was used to delineate the 2008 ice margin. Comparison of the 2002 and 2008 outlines clearly shows the reduction in the ice-covered area during this 6-year period.

According to the LiDAR measurements, the surface elevation of the ice cap ranges from 637 m a.s.l. at the margin of the Blágilsjökull NW outlet to 1443 m a.s.l. on an ice-free nunatak in the middle of the ice cap. The highest snow-covered point on the ice cap reached an elevation of 1428 m a.s.l. at the time of the LiDAR measurements in September 2008. The altitude of the summit of Snæfellsjökull is given as 1446 m a.s.l. on the AMS maps of Iceland based on a geodetic measurement of the highest point of the very steep central nunatak, which is likely to have been snow-free at the time of the measurement. The spacing of the LiDAR point measurements on the highest part of the ice cap is ~ 2 m so that it is likely that the very highest point of the steep nunatak was not captured by the LiDAR measurements. Therefore, the highest point on Snæfellsjökull may in fact be closer to traditional value of 1446 m a.s.l. rather than 1443 m a.s.l. as obtained by the LiDAR.

THINNING OF THE ICE CAP FROM 1999 TO 2008

The difference of the DTMs from 1999 and 2008 (Figure 6) shows that the greatest thinning has taken place near the ice margin, up to 40 m in some areas. The average lowering of the ice surface within the 2002 outline is 13 m. The thinning is smallest near the summit of the ice cap where it is found to be ~ 5 m on average above 1300 m a.s.l. over the nine-year period. The thinning is also relatively small near the

ice margin where the ice thickness in 1999 was small and the terminus has subsequently retreated, exposing new ice-free land. The average thinning within the area enclosed by the 2002 outline may give a misleading indication of the average negative mass balance of the ice cap in 1999–2008 because the area of ice cap was reduced from ~ 12.5 km² (the area in 1999 was most likely similar as in 2002, see Figure 2) to 10.0 km². Much of the ice-volume reduction, therefore, took place when the area of the ice cap was considerably smaller than 12.5 km². If the ice-volume reduction from 1999 to 2008 is divided by the average of the areas in 2002 (considering it a rough estimate of the area in 1999) and in 2008, one finds an average lowering of 14.5 m. This may, on the other hand, lead to an overestimate of the magnitude of the (negative) mass balance because the area of the ice cap did probably not change much between 1999 and 2002. Weighting the areas in 2002 and 2008, to take the comparatively slow initial retreat of the ice margin before 2002 into account, leads to the estimate that the average thinning of the ice cap between 1999 and 2008 was close to 14.0 m, that is 1.5 m_{ice} or 1.4 m_{w.e.} per year.

An attempt was made to construct similar elevation difference maps from DTMs created from the contours by Hnit hf. based on aerial photographs from 1979 and the contours from the AMS maps based on aerial photographs from 1946. However, the shape of the obtained elevation differences was not consistent with likely changes in the surface geometry of the ice cap, with widely varying elevation differences along similar elevations around the upper part of the ice cap indicating that the problems of measuring elevations of snow covered surfaces by traditional photogrammetric methods led to substantial errors in the 1979 and 1946 DTMs. It should also be noted that the 1979 contours by Hnit hf. have a 100 m vertical spacing on the ice cap so that it is difficult to derive an accurate DTM from them due to the coarse spacing.

As mentioned above, the average ice thickness of Snæfellsjökull is only 30 m according to radio-echo soundings in 2003. Most of the ice cap is likely to disappear within a few decades if the warm climate of Iceland in recent years persists. The ice thick-

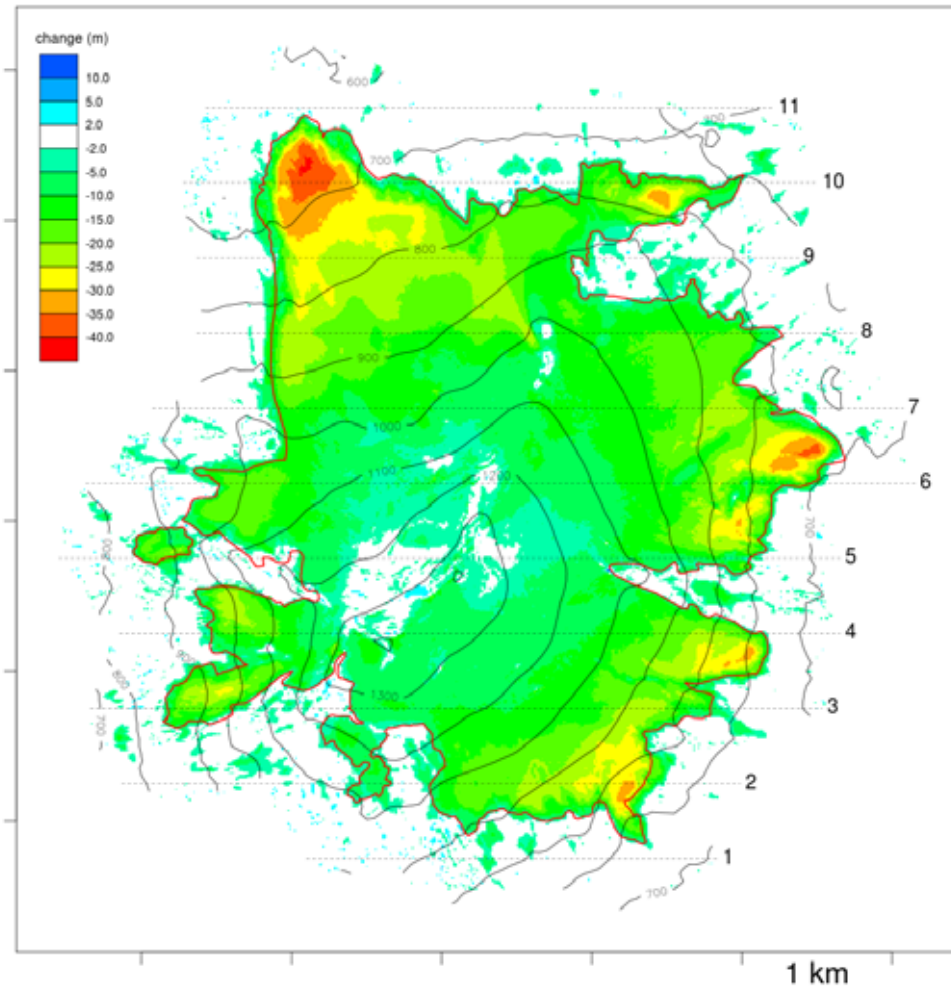


Figure 6. Change in the surface elevation of Snæfellsjökull from 1999 to 2008 (area 12.5 km² in 2002 and 10.0 km² in 2008). The red curve shows the ice margin in 2002. Dashed thin lines show the location of W–E profiles across the ice cap that are drawn in Figure 4. – *Hæðarbreyting Snæfellsjökuls (flatarmál jökulsins var 12.5 km² árið 2002 og 10.0 km² árið 2008) frá 1999 til 2008. Rauði ferillinn sýnir legu jökuljaðarsins árið 2002. Slitnar línur sýna staðsetningu sniða þvert yfir jökulinn frá vestri til austurs sem sýnd eru á 4. mynd.*

ness is variable, with relatively large areas with less thickness than 10–20 m. The ice is thicker in the main outlet tongues of Blágilsjökull, Jökulháls and Hyrningsjökull and directly to the west and east of the summit where ice thicknesses greater than 40–50 m were measured by Davíðsdóttir and co-workers (2003). The downwasting of the areas where the ice is thinnest is likely to produce areas of inactive ice that

will waste down more quickly than the rest of the ice cap as has already happened on the northeastern side of Snæfellsjökull where a part of the glacier below the equilibrium line became detached between 2002 and 2008 as seen on Figure 5 (right). The uppermost areas and those with the thickest ice will last longer but may be split into several smaller patches as the thin-ice areas become ice-free.

SENSITIVITY OF THE ICE CAP TO CLIMATE VARIATIONS

Annual mean summer temperature (May–Sept.) and annual accumulated precipitation (Oct.–Sept.) since 1930 at the weather station Stykkishólmur, on the north side of the Snæfellsnes peninsula, about 60 km from the ice cap, is shown on Figure 7. The terminus variations of Hyrningsjökull (Figure 2) and other information about variations in the size of the ice cap during the 20th century indicate that Snæfellsjökull was close to equilibrium in the period 1991–2000 when the advance of the period 1970–1995 was coming to an end and the retreat since 1995 was setting in. The variations of Hyrningsjökull also indicate that the ice cap was close to balance in the longer period 1981–2000 during which most glaciers in Iceland were comparatively close to being in equilibrium with the climate (Jóhannesson *et al.*, 2007). The average

temperatures of the periods 1981–2000, 1991–2000 and 2000–2008 are shown on Figure 7. The difference in mean summer temperature of the period 2000–2008 with respect to the earlier periods is 0.93 and 0.65°C, respectively. The precipitation time-series does not indicate a significant difference in precipitation between the periods so it appears that the ice volume reduction shown on Figure 6 has been driven by the warming that has taken place since the middle of the 1990s.

A quantitative analysis of the loss of ice volume between 1999 and 2008 must take into account the difference in timing within the year of the aerial surveys in 1999 and 2008, which took place in early August and early September, respectively. Lack of mass balance information for Snæfellsjökull makes it necessary to estimate the effect of this difference in timing indirectly based on the temperature time-series

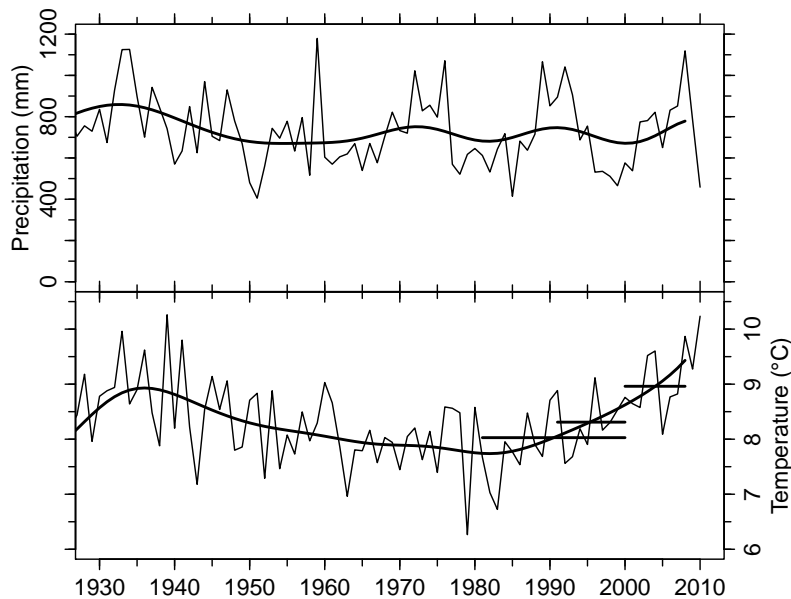


Figure 7. Summer temperature (May–September average) and annual precipitation (sum from October of the previous year to September) at Stykkishólmur, W-Iceland, from 1930 to 2010. Thick curves show weighted 10-year running means. The horizontal lines in the temperature panel denote the average temperature of the periods 1981–2000, 1991–2000 and 2000–2008. – *Sumarhiti (meðaltal maí til september) og ársúrkoma (summa frá október fyrra árs til september) í Stykkishólmi 1930 til 2010. Breiðir ferlar sýna vegið 10 ára meðaltal. Meðalhiti tímabilanna 1981–1999, 1991–1999 og 2000–2008 er sýndur með breiðum, láréttum strikum.*

from Stykkishólmur. This may be crudely done by assuming that the ice cap was approximately in balance on average in the period 1991–2000 (based on the relatively small terminus variations in this time period, see Figure 2) and that total summer melting can be estimated by the degree–day sum near the average altitude of the ice cap, which is close to 1000 m a.s.l. (assuming a vertical temperature lapse rate of 0.6°C per 100 m). The ice volume reduction between 1999 and 2008 is assumed to be due to the total degree–day sum of this period in excess of the sum corresponding to the mean climate of 1991–2000. The melting from 5 August to 2 September 1999 may then be estimated proportionally from the degree–day sum of this 28-day long period and is found to be approximately 1.4 m of ice. This estimate can be made more accurate by using the actual distribution of elevation of the ice surface but this is not considered necessary for the purpose of the study presented here since the result is not sensitive to the assumed elevation for the degree–day calculations. Using 800 m a.s.l. instead of 1000 m does not alter the estimated value of the melting over this period by more than 0.1 m of ice.

These considerations are based on the assumption that changes in the extent and thickness of snow and firn can be ignored so that changes in ice surface elevation may be assumed to reflect changes in the volume of glacier ice of density 900 kg m^{-3} (Sorge’s law, see *e.g.*, Paterson, 1994). The average degree–day coefficient implied by these calculations is found to be approximately $8\text{--}10\text{ mm}_{\text{w.e.}}\text{ }^\circ\text{C}^{-1}\text{ d}^{-1}$ (depending slightly on the assumed elevation for the degree–day calculations), which is rather high compared with degree–day coefficients found in mass balance modelling of the large Icelandic ice caps ($\sim 5\text{ mm}_{\text{w.e.}}\text{ }^\circ\text{C}^{-1}\text{ d}^{-1}$ for snow, $5\text{--}8\text{ mm}_{\text{w.e.}}\text{ }^\circ\text{C}^{-1}\text{ d}^{-1}$ for ice, *cf.* Jóhannesson *et al.*, 2007, and references therein). This could be due to the rather dark surface of the ice cap due to dust blown from neighbouring ice-free areas.

The ice volume reduction of Snæfellsjökull in the period 1999 to 2008 is found to correspond to an annual average mass loss of $1.25\text{ m}_{\text{w.e.}}$ per year in this nine-year period, when correction is made for the difference in the timing of measurements in 1999 and

2008 and for the reduction in the ice-covered area during the period. This is somewhat lower than the $1.5\text{--}1.8\text{ m}_{\text{w.e.}}$ per year mass loss found by Guðmundsson *et al.* (2010) for the comparatively small Eyjafjallajökull, Tindfjallajökull and Torfajökull ice caps for the period 1998–2004, and similar to the mass loss of the large ice caps Langjökull, Hofsjökull and Vatnajökull in recent years, which was 1.4, 0.9 and $0.8\text{ m}_{\text{w.e.}}$ per year, respectively, in 2000–2008 according to mass balance measurements (Björnsson and Pálsson, 2008; Sigurðsson *et al.*, 2004; unpublished data from IES and IMO). The volume reduction of Snæfellsjökull corresponds to a mass-balance sensitivity of $-1.9\text{ m}_{\text{w.e.}}\text{ a}^{-1}\text{ }^\circ\text{C}^{-1}$, which also is somewhat lower in magnitude than -2 to $-3\text{ m}_{\text{w.e.}}\text{ a}^{-1}\text{ }^\circ\text{C}^{-1}$, that Guðmundsson and others found for Eyjafjallajökull, Tindfjallajökull and Torfajökull but larger than what has been estimated for the large ice caps of Iceland for which sensitivities in the range -0.5 to $-1.3\text{ m}_{\text{w.e.}}\text{ a}^{-1}\text{ }^\circ\text{C}^{-1}$ have been estimated (Jóhannesson, 1997; Aðalgeirsdóttir *et al.*, 2006).

AUTOMATED MAPPING OF CREVASSES

As mentioned above, crevasses can be clearly seen on hillshades of the LiDAR DTM. An attempt was made to identify the location of crevasses with a digital procedure based on the calculation of the local curvature of the DTM. Crevasses are linear features in the DTM characterised by a locally high curvature transverse to the strike of the crevasse compared with a much lower curvature along the direction of the crevasse. As crevasses can strike in many directions it is not sufficient to compare the curvature of the ice surface in the x - and y -directions, $\partial^2 z_s / \partial x^2$ and $\partial^2 z_s / \partial y^2$. A more general procedure allowing for any crevasse direction must be employed. This can be done by calculating the eigenvalues λ_1 and λ_2 of the curvature matrix

$$S = \begin{bmatrix} \frac{\partial^2 z_s}{\partial x^2} & \frac{\partial^2 z_s}{\partial x \partial y} \\ \frac{\partial^2 z_s}{\partial x \partial y} & \frac{\partial^2 z_s}{\partial y^2} \end{bmatrix} \quad (1)$$

of the ice surface elevation z_s .

The larger eigenvalue λ_1 will be equal to the second derivative of the ice surface $\partial^2 z_s / \partial \xi^2$ in the direction in which this derivative reaches maximum and λ_2 will be the second derivative $\partial^2 z_s / \partial \eta^2$ in the direction of the minimum of the derivative. These directions, which are the eigenvectors of the matrix S , are always orthogonal to each other so that ξ and η may be considered coordinates in a rotated coordinate system with the ξ -axis transverse to the crevasse and η -axis along the crevasse.

The crevasse detection procedure proposed here involves comparing the maximum curvature, λ_1 , and the difference between the curvatures in the ξ - and η -directions, $\lambda_1 - \lambda_2$, to thresholds chosen by trial and error to identify points in the DTM that are likely to lie along crevasses. The thresholds $\lambda_1 > 0.03 \text{ m}^{-1}$ and

$\lambda_1 - \lambda_2 > 0.02 \text{ m}^{-1}$ were found to delineate most of the crevasses that can be located by visual inspection of the hillshade of the glacier surface (Figure 8).

As expected, many of the crevasses are perpendicular to the direction of the ice flow and there are crevasses pointing upstream near the lateral margins of outlet glaciers. The most impressive crevasse fields are likely to be related to ice flow over irregularities in the bottom topography.

The results of the crevasse detection algorithm are shown in more detail on Figure 8 which shows the calculated direction along the identified crevasses as line segments as well as the location of points near crevasses as in Figure 8. The line segments are drawn in the direction of the eigenvector corresponding to the smaller one of the two eigenvalues of the curvature

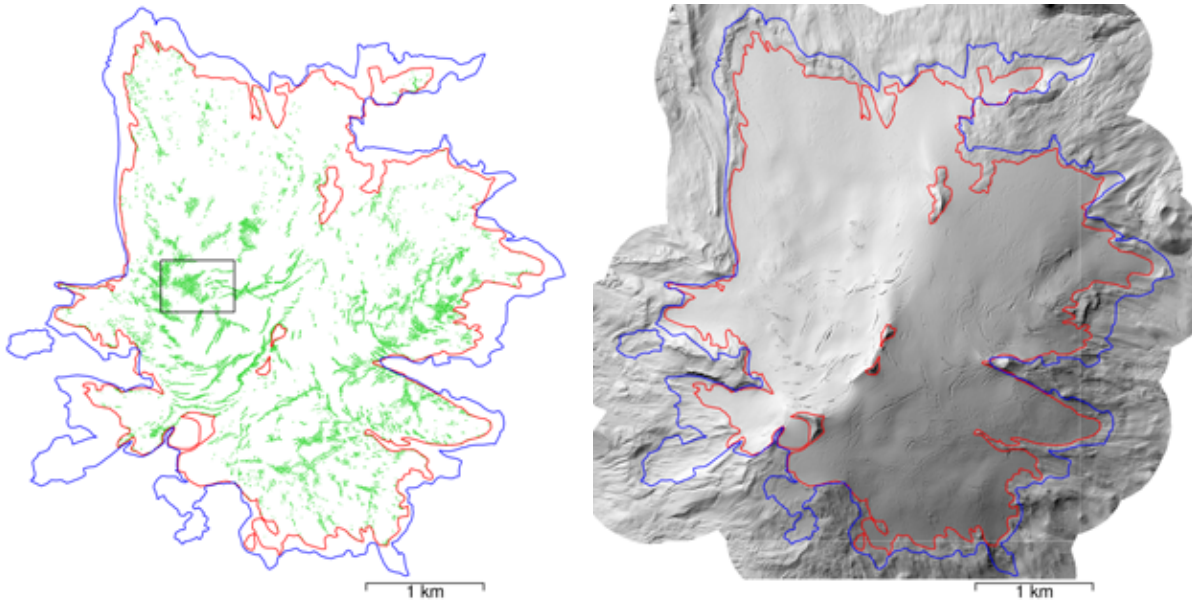


Figure 8. Left: Location of crevasses delineated by an digital analysis of the 5x5 m LiDAR DTM from 2008 (see text for explanation). The box shows the location of the crevassed area shown in Figure . Right: A hillshade of the LiDAR DTM showing many crevasses. The glacier margin in 2008 as delineated from the LiDAR measurements and the 2002 margin measured by GPS are shown with red and blue curves, respectively. – *Vinstri mynd: Staðsetning sprungna ákvörðuð með greiningu á 5x5 m LiDAR landlíkaninu frá 2008 (sjá frekari útskýringar í texta). Hægri mynd: Skygging á LiDAR landlíkaninu sem sýnir margar sprungur. Útlína jökulsins frá 2008 dregin á grundvelli LiDAR mælingarinnar er sýnd með rauðri línu og útlínan frá 2002 með blárrí línu.*

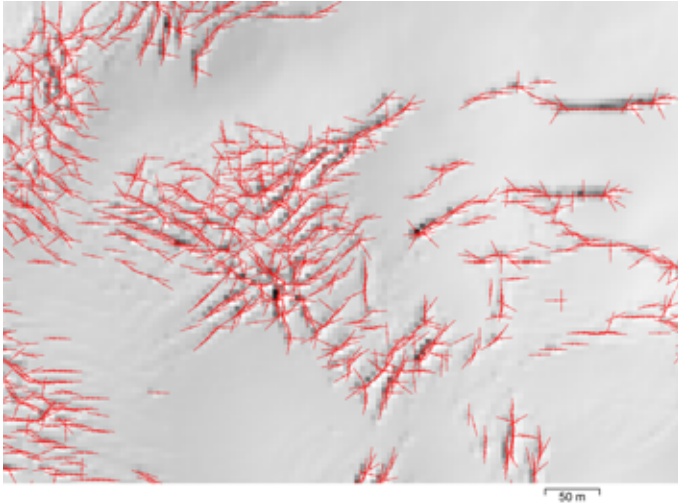


Figure 9. A zoom-in of the hillshade of the LiDAR DTM showing an area with many crevasses (the location of the area is shown with a box on Figure 8) and the location of points identified as being near a crevasse. Line segments show the calculated direction along the crevasse which is the direction of the eigenvector corresponding to the smaller eigenvalue λ_2 of the curvature matrix (1) (see text for explanation). – *Sprungusvæði á vestanverðum Snæfellsjökli. Punktar sýna sjálfvirk ákvarðaða staðsetningu sprungna og línur reiknaða sprungustefnu. Staðsetning svæðisins er sýnd með ramma á 8. mynd.*

matrix, λ_2 , that is in the direction of the η -axis of the rotated coordinate system described above. The figure shows that the calculated directions of the crevasses are in most cases consistent along the sequence of points that correspond to the same crevasse, although some irregularities are also evident, especially near the end of crevasses. Further evaluation of this procedure on other ice caps and glaciers is needed before it can be routinely used for crevasse detection but these initial results are encouraging.

Finally, it should be noted that the results of any mapping of crevasses must be used with caution as crevasses may be hidden by snow at the time of the measurement of the glacier. Crevasses also move with the ice and may open up in new locations. In particular, new crevasse fields are often created by surges and other accelerations of the ice flow. Thus, mapped crevasses are an indicator of potential danger for travellers on the glacier but absence of mapped crevasses in an area cannot be considered as evidence that passage through the area is safe.

Acknowledgements

Financial support for LiDAR mapping of glaciers in Iceland has been provided by RANNIS (The Icelandic Centre for Research), Landsvirkjun (the National Power Company of Iceland), the Icelandic

Public Road Administration, the Reykjavík Energy Environmental and Energy Research Fund, the National Land Survey of Iceland, the Icelandic Ministry for the Environment and the Klima- og Luftgruppen (KoL) research fund of the Nordic Council of Ministers. This publication is contribution number 3 of the Nordic Centre of Excellence SVALI, “Stability and Variations of Arctic land Ice”, funded by the Nordic Top-level Research Initiative (TRI). An orthorectified SPOT5 HRG image (© CNES/SPOT Image Corporation) was provided by the National Land Survey of Iceland. Bjarni Reykr Kristjánsson provided the 2002 glacier outline measured by GPS.

ÁGRIP

Yfirborð Snæfellsjökuls var kortlagt árið 2008 með leysimælingu úr flugvél. Samanburður við loftmyndakort frá 1999 gefur til kynna að jökullinn hafi lækkað um 14.0 m að meðaltali á þessu níu ára tímabili. Það svarar til rýmnunar um $1.25 \text{ m}_{\text{vatns}}$ á ári að meðaltali á þessu tímabili þegar leiðrétt hefur verið fyrir mismunandi tímasetningu mælinganna innan ársins. Flatarmál jökulsins minnkaði úr 12.5 km^2 árið 2002 niður í 10.0 km^2 árið 2008. Næmi jökulsins fyrir hitabreytingum var metið $-1.9 \text{ m}_{\text{vatns}} \text{ a}^{-1} \text{ } ^\circ\text{C}^{-1}$ út frá hitamælingum í Stykkishólmi. Það er svipað gildi og reiknað hefur fyrir nokkra aðra íslenskra jökla á síðari ár-

um. Meðalþykkt Snæfellsjökuls er einungis 30 m. Því má ætla að jökullinn hverfi að mestu á fáum áratugum héðan í frá ef loftslag verður áfram jafn hlýtt og verið hefur á undanförunum árum. Kortið frá 2008 hefur verið notað til þess að staðsetja sprungur á yfirborði jökulsins með sjálfvirkri aðferð sem byggir á greiningu á krappa yfirborðsins.

REFERENCES

- Aðalgeirsdóttir, G., T. Jóhannesson, H. Björnsson, F. Pálsson and O. Sigurðsson 2006. The response of Hofsjökull and southern Vatnajökull, Iceland, to climate change. *J. Geophys. Res.* 111, F03001, doi: 10.1029/2005JF000388.
- Bahr, D. B., M. F. Meier and S. D. Peckham 1997. The physical basis of glacier volume–area scaling. *J. Geophys. Res.*, 102, 20,355–20,362.
- Björnsson, H. 1978. The surface area of glaciers in Iceland. *Jökull* 28, 31.
- Björnsson, H. and F. Pálsson 2008. Icelandic glaciers. *Jökull* 58, 365–386.
- Davíðsdóttir, M. 2003. *Íssjármæling Snæfellsjökuls. (Radio echo-sounding of Snæfellsjökull)*. BS thesis, University of Iceland, 44 pp.
- Guðmundsson, S., H. Björnsson, E. Magnússon, E. Berthier, F. Pálsson, M. T. Guðmundsson, Þ. Högnadóttir and J. Dall 2010. Response of Eyjafjallajökull, Torfajökull and Tindfjallajökull ice caps in Iceland to regional warming, deduced by remote sensing. *Polar Research* 30, 7282, doi: 10.3402/polar.v30i0.7282.
- Jóhannesson, T. 1997. The response of two Icelandic glaciers to climate warming computed with a degree-day glacier mass-balance model coupled to a dynamic model. *J. Glaciol.* 43, 321–327.
- Jóhannesson, T., G. Aðalgeirsdóttir, H. Björnsson, P. Crochet, E. B. Elíasson, S. Guðmundsson, J. F. Jónsdóttir, H. Ólafsson, F. Pálsson, Ó. Rögnvaldsson, O. Sigurðsson, Á. Snorrason, Ó. G. Blöndal Sveinsson and Th. Thorsteinsson 2007. *Effect of climate change on hydrology and hydro-resources in Iceland*. Reykjavík, National Energy Authority, Rep. OS-2007/011, 91 pp.
- Kristjánsson, L. and T. Jónsson 1998. Alþjóða-heimskautaárin tvö og rannsóknastöðin við Snæfellsjökul 1932–33. (The two International Polar Years and the field research station at Snæfellsjökull, W-Iceland, in 1932–33). *Jökull* 46, 35–47.
- Paterson, W. S. B. 1994. *The Physics of Glaciers*, 3rd ed. New York, Elsevier, 480 pp.
- Sigurðsson, O. 1998. Glacier variations in Iceland 1930–1995. *Jökull* 45, 3–25.
- Sigurðsson, O. 2009. Glacier variations 1930–1970, 1970–1995, 1995–2006 and 2006–2007. *Jökull* 59, 103–108.
- Sigurðsson, O. and T. Jóhannesson 1998. Interpretation of glacier variations in Iceland 1930–1995. *Jökull* 45, 27–33.
- Sigurðsson, O., Th. Thorsteinsson, S. M. Ágústsson and B. Einarsson 2004. *Afkoma Hofsjökuls 1997–2004. (Mass balance of Hofsjökull 1997–2004)*. Reykjavík, National Energy Authority, Rep. OS-2004/029, 54 pp.
- TU-Vienna-IPF. 2002. *SCOP. General Information*. Institut für Photogrammetrie und Fernerkundung. Web-page dated 9 December 2002, accessed 8 March 2010: “http://www.ipf.tuwien.ac.at/products/produktinfo/scop/englisch/scop_e.html” and “http://www.ipf.tuwien.ac.at/products/produktinfo/scop/englisch/scop_basic_e.html”.
- Zingg, Th. 1941. Die Polarstation Snæfellsjökull 1932/33. In: *Année Polaire Internationale 1932–33. Participation Suisse*. Publication de la Station centrale suisse de Météorologie à Zürich. 22 pp., 69 pp. of tables and 6 pp. of graphs.